Title

Dislocation structure and deformation in iron processed by equal-channel-angular pressing

Journal

Metallurgical and Materials Transactions A-Physical Metallurgy and Materials Science, 35A(4)

ISSN

1073-5623

Authors

Han, B Q
Lavernia, E J
Mohamed, F A

Publication Date

2004-04-01

Peer reviewed

Dislocation Structure and Deformation in Iron Processed by Equal-Channel-Angular Pressing

BING Q. HAN, ENRIQUE J. LAVERNIA, and FARGHALLI A. MOHAMED

The evolution of dislocation structure in pure Fe during equal-channel-angular pressing (ECAP) is investigated. Also, the effect of the formation of this dislocation structure on deformation and fracture behavior is examined. The results show that intensive dislocation cell blocks are present after one pass and even more after subsequent pressings. The low-energy dislocation structures (LEDS) may have changed into the high-energy dislocation structures (HEDS) in the final several pressings. The high-density array of dislocations plays a significant role in strengthening. The HEDS may cause the materials to lose work-hardening ability and show a cleavage morphology of the fracture surface. A proper subsequent annealing treatment will lead to the evolution of HEDS to LEDS while maintaining little grain growth. This change in the nature of dislocation structures allows ultrafine-grained materials to achieve an excellent combination of high strength and high ductility.

I. INTRODUCTION

EQUAL-CHANNEL angular pressing (ECAP) is a processing technique that is capable of producing ultrafine-grained (UFG) materials with grain sizes of 200 to 500 nm.[1] During ECAP, the material is pressed through a die that has two channels containing the same cross section with an angle of 90 deg or higher. In each pass, large shear deformation is introduced into materials. This processing technique possesses some advantages over several other processing techniques, including the consolidation of mechanically alloyed (MA) powders, heavy cold work or high-pressure torsion. Consolidation of MA powders is an effective approach to manufacturing nanostructured or UFG materials. However, bulk MA alloys contain residual porosity and impurities that will influence mechanical performance.[2,3] While extensive cold deformation can also be used to produce large amounts of UFG materials, such materials often contain a cellular substructure in which grain boundaries (GBs) have low-angle misorientations, causing anisotropy of mechanical properties.[4,5] The high-pressure torsion technique is one of the most effective processing techniques for producing nanostructured materials (grain sizes $<$ 100 nm).[6,7] However, the amount of pressed materials is generally very small. Moreover, this approach requires equipment that is capable of generating large pressures, which can be a technological obstacle for extensive application in industry. Therefore, it is difficult to scale this approach up for mass production for grain refinement. Comparatively, ECAP can be used to produce large amounts of porosity-free and impurity-free bulk UFG materials with GBs having high-angle misorientations.

Early investigations using ECAP processing extensively focused on aluminum or copper alloys.[1] Very recently, significant interest has shifted to the use of ECAP in processing UFG low-carbon steels. This interest has been motivated in part by the fact that UFC low-carbon steels can be used in many applications as a structural material[8–12] and in part by the characteristic that ECAP can improve the strength of materials without a need to change their chemical composition. In related studies, Shin and co-workers[9,11] processed carbon steel (Fe-0.15 pct C-0.25 pct Si-1.1 pct Mn) *via* ECAP and used four passes at 623 K. A tensile strength of 940 MPa was obtained from tensile testing on near standard specimens with equiaxed ultrafine grains of 0.2 μm. Most recently, the microstructure and mechanical properties of another low-carbon steel (Fe-0.08 pct C-0.18 pct Si-0.42 pct Mn) processed *via* ECAP were investigated.[12] It was observed that the ultimate tensile strength (UTS) increased with increasing number of passes. Also, a value higher than 800 MPa was achieved after three passes although the grain size of ferrite phase after three passes was found to be essentially the same as that of one pass, close to 200 nm.

Despite the aforementioned recent studies on UFG low-carbon steels and the implications of their results, the deformation behavior of these alloys with grain sizes of about 200 nm is not fully understood, largely due to complexities associated with their complicated chemical composition. In order to obtain baseline information that can shed light on the origin of deformation processes operating in UFG low-carbon steels, it is essential, as a first step, to investigate the deformation behavior of UFG pure Fe. Such baseline information can be used in future investigations on UFG steels to identify the effects of the presence of alloying elements in Fe on deformation and fracture processes.

In an earlier investigation,[13] the present authors investigated pure Fe processed by ECAP. The investigation focused on the deformation behavior of pure Fe, which was characterized by an average grain size of 200 nm obtained after eight passes. The results showed that UFG Fe exhibited high strength and that localized necking occurred during deformation. However, in that investigation,[13] no detailed examination of the microstructure of UFG pure Fe resulting from ECAP processing and subsequent mechanical testing was carried out to assess the influence of dislocation structure on mechanical properties of the material.

BING Q. HAN, Assistant Researcher, Department of Chemical Engineering and Materials Science, and ENRIQUE J. LAVERNIA, Dean, College of Engineering, are with the University of California, Davis, CA 95616. Contact e-mail: bqhan@ucdavis.edu FARGHALLI A. MOHAMED, Professor, is with the Department of Chemical Engineering and Materials Science, University of California, Irvine, CA 92697.

Manuscript submitted April 24, 2003.

In the present study, the evolution of microstructure during the ECAP processing and subsequent deformation of pure Fe was investigated by means of transmission electron microscopy, tensile testing, and scanning electron microscopy. It is the purpose of this article to report and analyze the results that revealed the underlying relationship between microstructure and mechanical properties.

II. MATERIALS AND EXPERIMENTAL PROCEDURE

A commercial grade of 99.95 pct Fe having a composition, in ppm, of Ni100, O86, Si75, Co34, Al27, N11, P4.8, Ge4.6, Cr4.3, Cu3.9, B2.8, Til.3, C<1, with the balance as Fe was used in the investigation. Before pressing, the annealing treatment of Fe was carried out at a temperature of 1203 K for 1 hour in an industrial vacuum furnace. The material was subjected to severe plastic deformation using ECAP at room temperature. The ECAP die had an internal angle of 90 deg between the two parts of the channel and an outer arc of curvature of ~20 deg, where these two parts intersect. During the pressing operation, each sample was rotated by 90 deg in the same direction between consecutive passes through the die. This procedure is generally termed processing route B_C. Further information can be found in the earlier investigation.[13]

Tensile flat dog-bone specimens with a gage length of 12 mm, a width of 3.6 mm, and a thickness of 1.6 mm were machined from the as-pressed billets with the gage sections lying parallel to the direction of pressing. Tension testing was performed using an Instron 8801 machine (Canton, MA) equipped with a dual-camera video extensometer. The load accuracy is 0.5 pct of the indicated load and the resolution of the video extensometer is approximately 5 μm. The sampling rate of data is chosen as 10 point/s. Tensile specimens were tested at a constant crosshead velocity of 0.012 mm/s until failure.

The microstructure was examined by a transmission electron microscopy (TEM) operated at 200 kV. The samples for TEM observations were prepared first by manually polishing until approximately 30 μm, then by dimpling for a thinned area, and finally by ion milling until a tiny perforation appeared in the center. The fracture surface of the tensile specimens was studied by a scanning electron microscope (SEM) operated at 10 kV.

III. EXPERIMENTAL RESULTS

A. *Tensile Behavior*

The tensile behavior of the annealed Fe and the ECAP Fe is shown in Figure 1 in the form of engineering stress as a function of engineering strain. The yield stress of the annealed Fe at a strain of 0.2 pct is 79 MPa. There is an extensive region of work hardening after yielding and a large elongation to failure for the annealed Fe. The plastic behavior of the ECAP Fe is noticeably different from that of the annealed Fe: the ECAP Fe exhibits a much higher tensile strength than that of the annealed Fe, with a concomitant loss of ductility. The yield strength and the UTS of the ECAP Fe after the fourth pass (ECAP-4 Fe) are approximately 696 and 723 MPa, respectively. Between those two points, there

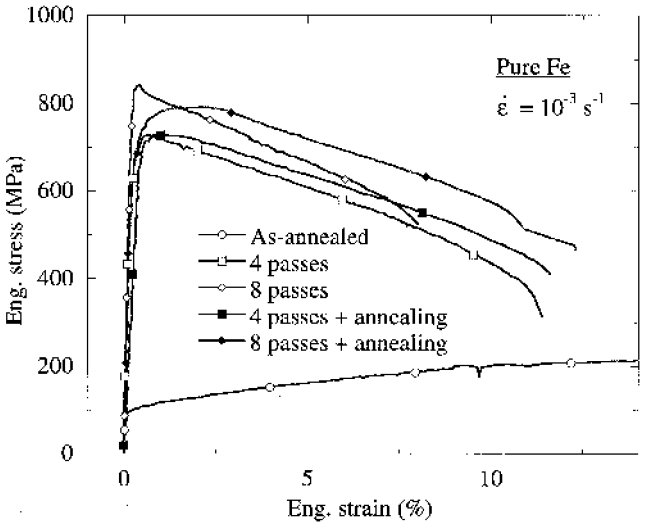

Fig. 1—The tensile engineering stress-strain of the as-annealed Fe, the as-pressed ECAP Fe, and the subsequent annealed ECAP Fe at 473 K for 1 h.

is a brief work-hardening region before necking. The UTS in the ECAP-Fe after the eighth pass (ECAP-8 Fe) increases to 840 MPa, more than 10 times stronger than annealed pure Fe. However, the ECAP-8 Fe does not exhibit any work hardening following yielding. Moreover, the material shows a continuous drop in the stress-strain curve, indicating the occurrence of necking immediately at the onset of yielding.

In order to understand the effect of annealing on mechanical properties, the ECAP-Fe subjected to annealing at 473 K for 1 hour and cooled in air to ambient temperature was also tested and the results were compared with those of the as-pressed Fe, as shown in Figure 1. A temperature of 473 K, which is much lower than the recrystallization temperature of Fe, is selected to make sure that the treatment occurs in the recovery region. It is observed that the stress-strain curve of the as-annealed ECAP-4 Fe is essentially the same as that of the as-pressed ECAP-4 Fe, but that of the as-annealed ECAP-8 Fe is remarkably different from that of the as-pressed ECAP-8 Fe. Although there is a slight reduction in yield strength and UTS, ductility of the as-annealed ECAP-8 Fe is much improved. Moreover, there is a work-hardening region after yielding.

B. *Microstructure*

The annealed pure Fe exhibits an equiaxed ferrite grain size of approximately 200 μm.[13] After pressing for the first pass, the prior coarse grains are optically found to be elongated along the pressing direction with the length of 200 to 500 μm and width of 30 to 90 μm. The angle between the longitudinal direction of the grains and the pressing direction is about 27.6 deg. After the second pass, the elongated grains are sheared into several shorter segments. After the fourth pass, the prior grains are sufficiently refined to render the grain boundaries indistinguishable under light microscopy analysis.

The microstructure of ECAP Fe was further examined by TEM. It is interesting to note that after the first pass, well-defined banded dislocation cell blocks (CBs) are formed in the microstructure, with the length and width of 0.5 to 1 μm and 0.15 to 0.4 μm, respectively, as shown in Figure 2(a).

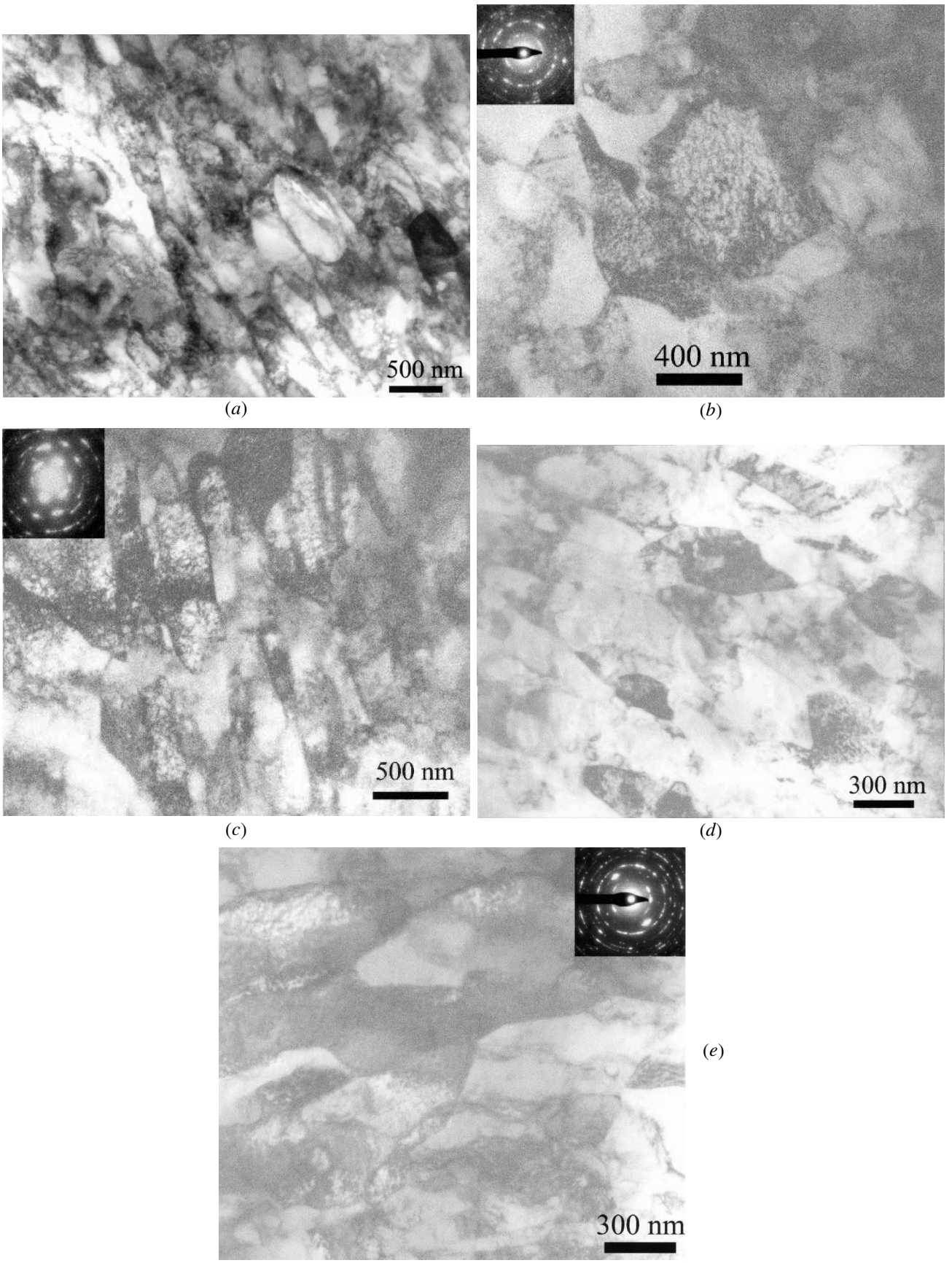

Fig. 2—TEM observation of microstructure after (*a*) one pass normal to the pressing direction, (*b*) two passes parallel to the pressing direction, (*c*) four passes normal to the pressing direction, and (*d*) eight passes normal to and (*e*) parallel to the pressing direction.

After two passes, the dislocations in CBs are more discernible (Figure 2(b)). Discontinuous circular rings in the selected-area electron diffraction (SAED) patterns, which were taken in an area with a diameter of about 2.5 μm, in the microstructure of Fe after two passes (ECAP-2 Fe) suggest that part of walls of dislocation CBs have evolved into GBs with high-angle misorientations, but dislocation CBs are distributed along several preferential directions. In the following passes, dislocation CBs in microstructure are further refined, as indicated by the presence of shorter length banded blocks. Furthermore, the length of the dislocation CBs decreases to approximately 0.5 μm after four passes in the transverse direction, although the width of the blocks has insignificant change, and is 0.13 to 0.34 μm, as shown in Figure 2(c). A high-density array of dislocations in blocks is observed. Moreover, reasonably high proportions of GBs with high-angle misorientations are observed since discontinuous circular rings in the SAED patterns, which were taken in an area with a diameter of about 1.5 μm, are observed. In the microstructure parallel to the pressing direction, dislocation CBs are quite similar to those normal to the pressing direction. The grain sizes are approximately 0.2 and 0.4 μm on the transverse and longitudinal cross sections, respectively.

The microstructure of the ECAP-8 Fe is shown in Figures 2(d) and (e). The grain size of ~200 nm after eight passes normal to the pressing direction is similar to that of a low-carbon Fe-0.15 pct C steel after four or eight passes at 623 K by Shin *et al.*[8,10] and a low-carbon Fe-0.08 pct C steel after three passes at 298 K by Fukuda *et al.*[12] Some elongated grains parallel to the pressing direction with dimensions exceeding 0.5 μm are also observed. There are also some finer grains with curved GBs in the ECAP-8 Fe. The circular rings in SAED patterns, which were taken in an area with a diameter of about 1.5 μm, suggest that there are high proportions of the GBs with high-angle misorientations. Inspection of the microstructure reveals that some grains contain more uniformly distributed dislocations with slightly lighter diffraction contrast and lattice distortions near the GBs. The observation suggests that the rearrangement of dislocations in the vicinity of GBs is completed, and some GBs may have evolved into nonequilibrium ones with high internal stress.

The microstructure of ECAP-4 Fe and ECAP-8 Fe subjected to annealing at 473 K for 1 hour is shown in Figure 3(a). Samples were taken parallel to the pressing direction. There are less dislocation CBs after annealing in the ECAP-4 Fe (Figure 3(a)). Moreover, straight GBs are revealed. A similar result was also observed in the ECAP-8 Fe (Figure 3(b)) after annealing. Dislocation CBs are observed and some grains with high-angle GBs contain a much lower density of dislocations. In both materials, slight grain growth was observed. The results suggest that dynamic recovery has partially occurred during annealing at 473 K for 1 hour.

C. *Fractography*

The as-annealed Fe exhibits a large uniform plastic deformation, manifested by a wavy morphology parallel to the loading direction. However, the necking deformation is observed on all ECAP Fe samples parallel to the tensile direction.

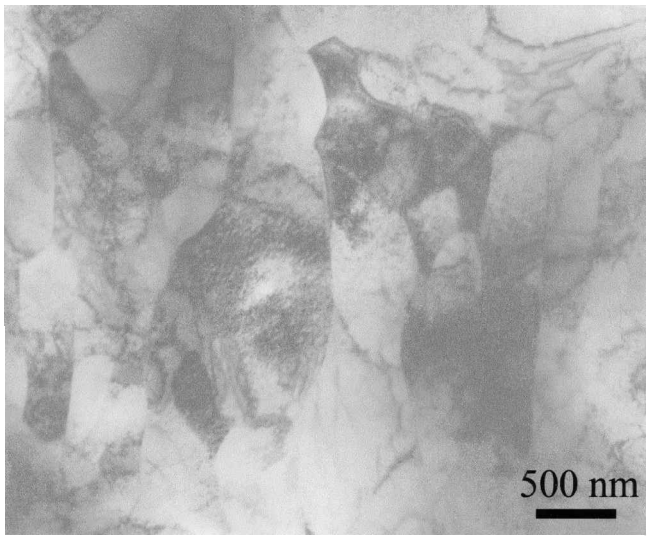

(*a*)

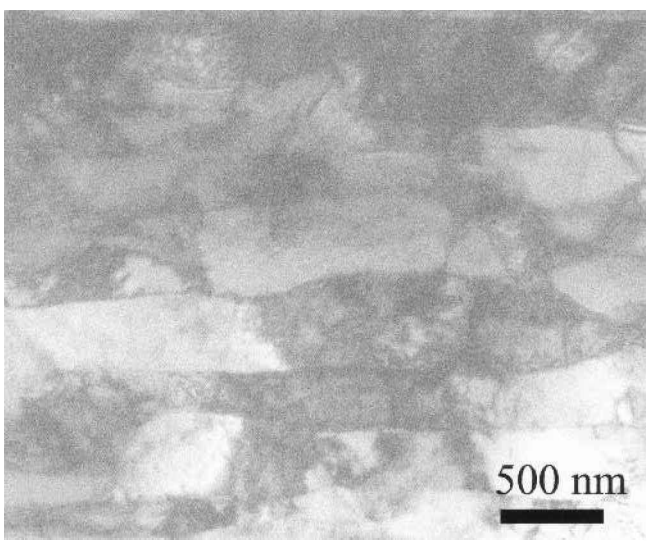

(*b*)

Fig. 3—TEM observation of the microstructure parallel to the pressing direction in (*a*) the ECAP-4 and (*b*) the ECAP-8 Fe after annealing at 473 K for 1 h.

Fractography of tensile specimens is examined by SEM, as shown in Figure 4. The fracture surface of the annealed Fe, shown in Figure 4(a), consists of ductile dimples with slip steps on the walls of dimples, indicative of intensive plastic deformation. The fracture surface of the ECAP-4 Fe (Figure 4(b)) consists of bimodal dimples. The large shallow poorly defined dimples have a size similar to those on the fracture surface of the as-annealed Fe, which might be developed from residual prior coarse grains. The small dimples (Figure 4(c)) have a size of approximately 1 μm, which might arise from dislocation CBs, which were developed during ECAP. The dimple morphology indicates that the ECAP-4 Fe still retains some work-hardening capacity, which is related to the dislocation activity.

The fracture surface of the ECAP-8 Fe, as shown in Figure 4(d), has veinlike patterns, reminiscent of fracture *via* cleavage. Inspection of the "cleavage" surface (Figure 4(e)) reveals

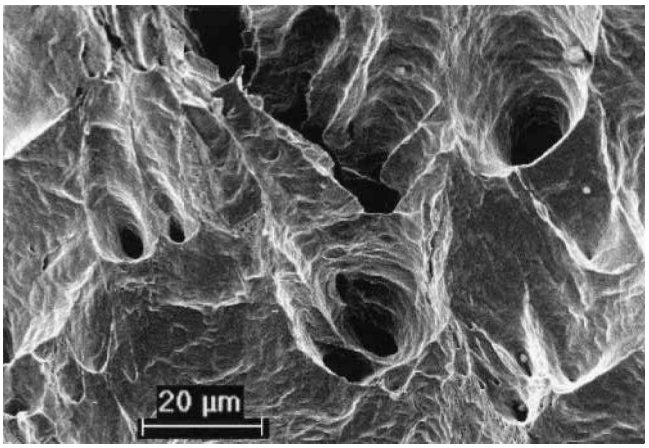

(*a*)

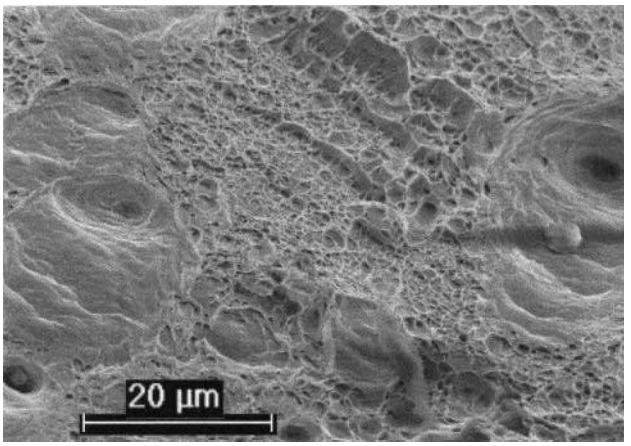

(*b*)

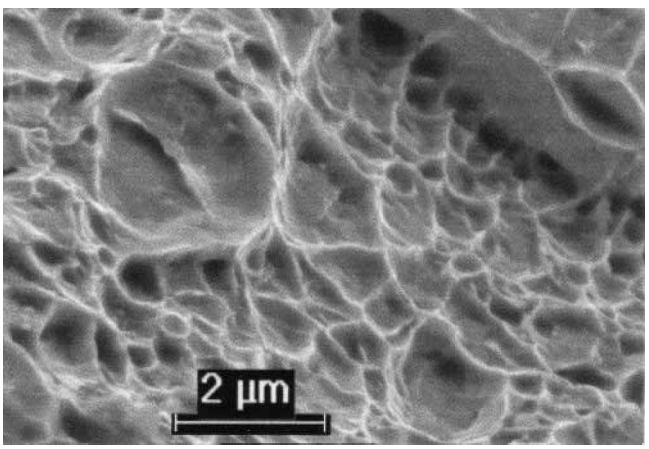

(*c*)

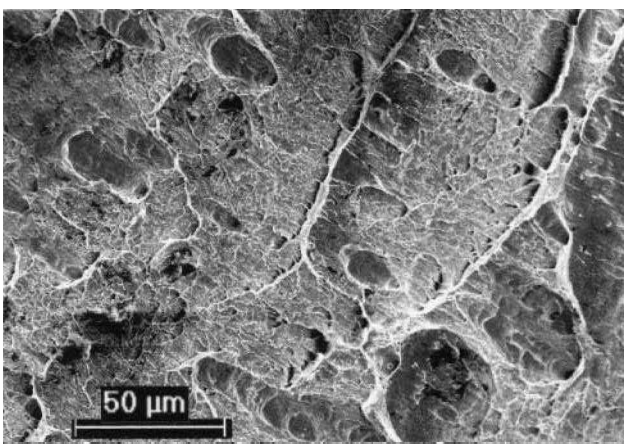

(*d*)

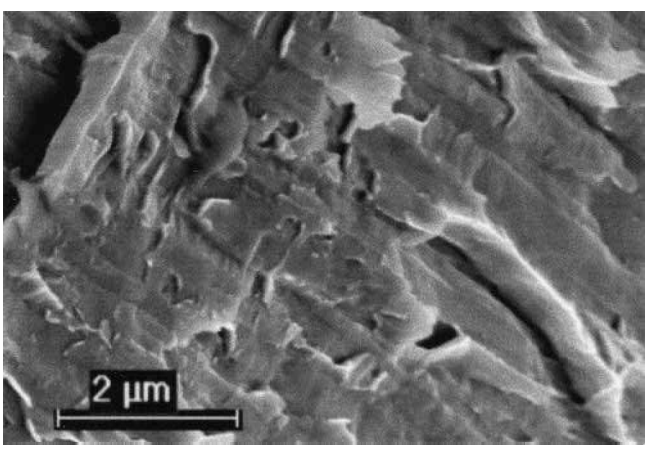

(*e*)

Fig. 4—Fractography of (*a*) the annealed Fe, (*b*) and (*c*) the ECAP-4 Fe, and (*d*) and (*e*) the ECAP-8 Fe.

that there is a subtle banding structure with a width of ~0.3 μm, which might be associated with well-defined substructures after eight passes. The veinlike patterns of tensile fracture surface in the ECAP Fe are similar to the steplike morphology of tensile fracture surface in a metallic glass tested at elevated temperatures[14] and a nanostructured Fe at ambient temperature.[15] The cleavage morphology indicates that the ECAP-8 Fe has very limited work-hardening capacity.

Fractography of tensile specimens of ECAP-Fe subjected to subsequent annealing is shown in Figure 5. Bimodal dimples are also observed on the fracture surface of the ECAP-4 Fe under subsequent annealing (Figure 5(a)), which are analogous to Figures 4(b) and (c), but with a deeper shape. Inspection of the fractography suggests that dislocations are able to move a longer distance during tension in the material subjected to subsequent annealing. It is interesting to note

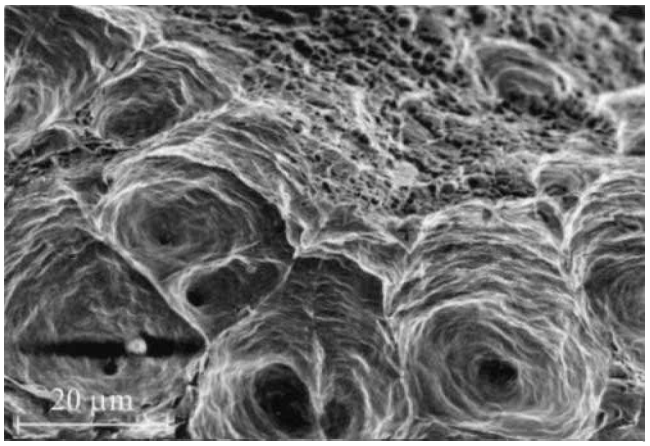

(*a*)

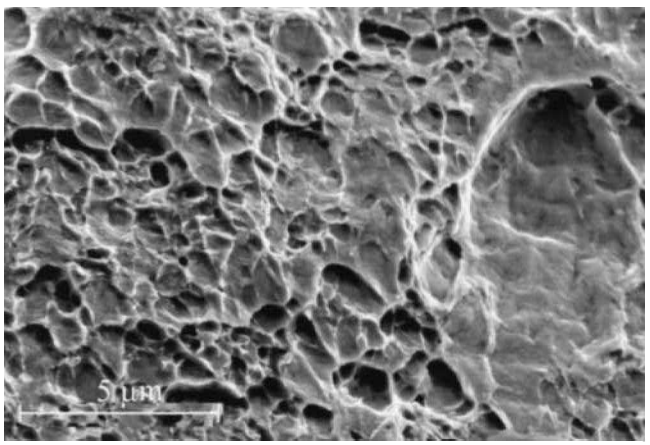

(*b*)

Fig. 5—Fractography of (*a*) the ECAP-4 Fe and (*b*) the ECAP-8 Fe after annealing at 473 K for 1 h.

that the morphology of fracture surface of the ECAP-8 Fe subjected to annealing is different. The veinlike patterns disappear, but a morphology with bimodal dimples emerges (Figure 5(b)), suggesting that considerable dislocation activity after annealing has been recovered.

IV. DISCUSSION

Dislocation structures and microstructural evolution during the cold deformation, mostly *via* rolling, of metals have been investigated intensively.[5,16] Dense dislocation walls (DDWs) are formed in grains at low strains, and further microbands (MBs), which contain a high density of dislocations, are formed. The DDWs and MBs, the geometry necessary boundaries for the subdivision of grains, surround blocks of equiaxed cells, the typical cell block structure in which there is a low density of dislocations. With the increasing frequency of MBs, the size of the ordinary cells decreases and the misorientation across the cell walls increases. With increasing strain, the dislocation boundaries reorient with an increasing tendency into a lamellar structure. The number of deformation-induced high-angle boundaries in a lamellar structure increases with increasing strain. In a typical lamellar structure at large strains, the lamellar boundaries' sandwich thin layers of cells and subgrains, which are oriented along the material flow direction. On the basis of the principle of low-energy dislocation structures (LEDS),[17,18] glide dislocation configurations (DDWs, MBs, and lamellar structure) reduce the energy in dislocation structures and increasingly approach the minimum energy per unit length of dislocation line as the density of dislocations increases. The LEDS theory can explain very well many phenomena in plastic deformation, for instance, four stages of work hardening and shape of stress-strain curve.

In the cold deformation by means of ECAP, a large shear strain of 1.15 per pass is introduced into the materials through two channels with 90 deg *via* dislocation slip.[19] Additionally, the length of lamellar structure is shorter than that from rolling. Inspection of the microstructure by TEM reveals that there are many dislocation CBs in the deformed prior grains after one pass and more dislocation CBs after two passes. With increasing strains, some dislocations around block walls may have been rearranged to form the dislocation boundaries with high-angle misorientations, leading dislocation CBs to a granular-type structure. The density of dislocations introduced by shear deformation increases dramatically in the initial several pressings and rapidly to a high level after four passes. As indicated by Figure 2(c), the low-energy dislocation CBs after four passes are available. Therefore, the deformation structures are still in thermodynamic equilibrium,[18] as manifested by the insignificant effect of subsequent annealing on tensile behavior. The dimpled fracture surface in ECAP-4 Fe suggests that there is a significant dislocation contribution to work hardening.

During the subsequent severe deformation from four to eight passes, the dislocation density gradually approaches saturation in the deformation structures. It may exist in more dislocations than required to accommodate the misorientations between walls of dislocation CBs. The dislocation structures after eight passes, termed the high-energy dislocation structures (HEDS), may be far from thermodynamic equilibrium since the dislocation CBs have evolved into a granular structure by rearrangement of walls of CBs. The excess dislocations at boundaries are not arranged in LEDS, which makes the subgrain boundary unstable. Although no attempt was made in the present investigation to examine the unstable boundary, evidence of the existence of nonequilibrium GBs in UFG materials processed by severe plastic deformation has been reported by using X-ray diffraction techniques and high-resolution electron microscopy.[1,20] The nonequilibrium GBs are characterized by the high density of trapped lattice dislocations and lattice distortion near the boundaries. There are more dislocations than required to geometrically accommodate the misorientations across the boundaries, leading to the high density of vacancy concentration and high long-range internal stresses in the vicinity of nonequilibrium GBs, which in turn have a significant effect on diffusion and plastic deformation.[1,21] Moreover, the long-range strain field energy of nonequilibrium GBs was found to be 2 times higher than that of equilibrium GBs.[21] Because of the saturation of dislocations and the existence of HEDS in the ECAP-8 Fe, the significant contribution of dislocation accumulation to work hardening was impeded, as evident by both the absence of work hardening in the stress-strain curve and the cleavagelike fracture surface.

To understand further the existence of HEDS, it is worth mentioning the results of thermal stability of nanostructured Fe prepared by mechanical attrition with annealing temperature.[22] The grain size and microstrain in nanostructured Fe powders annealed for 80 minutes at each temperature were analyzed by X-ray diffraction pattern. It is found that the microstrain decreases rapidly at temperatures below 473 K, while the grain size remains nearly constant. At temperatures higher than 573 K, the microstrain decreases linearly with increasing temperatures, while the grain growth is significant. The reduction of the microstrain at temperatures below 473 K is most probably attributed to the relaxation of HEDS. At temperatures higher than 473 K, the reduction is a result of grain growth.

A high-density array of dislocation CBs after ECAP is expected to lead to a significant dislocation strengthening in the ECAP processed material. This strengthening component can be expressed by $\Delta\sigma_{\perp} = M \cdot \alpha \cdot G \cdot b \cdot \rho^{1/2}$, where $M = 2.75$ is Taylor orientation factor for a bcc structure, and $\alpha = 0.4$ for bcc metals.[23] In the present study, the $\Delta\sigma_{\perp}$ values between the annealed Fe and the ECAP-4 Fe and between the annealed Fe and the ECAP-8 Fe are 617 and 761 MPa, respectively. If G of 64,000 MPa and b of $2.48 \cdot 10^{-10}$ m for α-Fe[24] are used, the increment of actual dislocation densities for ECAP-4 Fe and for ECAP-8 Fe can be estimated to be about $1.25 \cdot 10^{15}$ and $1.9 \cdot 10^{15}$ m^{-2}, respectively. The values are in good agreement with the results of the density of dislocations in other steels processed *via* severe plastic deformation.[6] The average dislocation lengths ($L = 1/\sqrt{\rho}$) in the ECAP-4 Fe and the ECAP-8 Fe are estimated to be 28.3 and 22.9 nm, respectively. Because of the heterogeneous distribution of dislocations, the actual dislocation length in the vicinity of GBs, especially nonequilibrium GBs, is much shorter. Although the difference of density of dislocations between ECAP-4 Fe and ECAP-8 Fe is small, the appearance of their fracture surfaces is considerably different. This can be attributed to the energy difference in their dislocation structures.

In the present study, after annealing at 473 K for 1 hour, the HEDS in the ECAP-8 Fe may have evolved into LEDS, as manifested by the dislocation-cell structures in the microstructure (Figure 3(b)), the existence of a brief work-hardening region in the stress-strain curve (Figure 1), and the dimpled fracture surface (Figure 5(b)). It is also observed that the subsequent annealing treatment has little effect on the plastic deformation of the ECAP-4 Fe, because of its stable LEDS. If the relaxation of HEDS in the ECAP-8 Fe is accomplished by diffusion through grain boundaries, the value of grain-boundary diffusivity ($D_b = \delta \cdot D_o \cdot \exp(-Q_b/RT)$) may be estimated using the following relationship regarding the relaxation time (t):[25]

$$t = \frac{0.03kTH^3}{G\Omega D_b \delta} \qquad [1]$$

where k is the Bolzmann constant, T is the absolute temperature, H is the distance at which the image of a dislocation disappears (≈30 nm[25]), G is the shear modulus of pure Fe, Ω is the atomic volume, and δ is the thickness of GBs. For $T = 473$ K, $G = 59{,}045$ MPa, $\Omega = 1.18 \cdot 10^{-29}$ m^3, $\delta \cdot D_o = 1.1 \cdot 10^{-12}$ m/s,[24] and $t = 3600$ s, the value of activation energy (Q_b) of grain-boundary diffusion during annealing is calculated to be 106.1 kJ/mol, which is smaller than 174 kJ/mol, the activation energy of grain-boundary diffusion in coarse-grained Fe.[24] The difference between the two values of the activation energy is not exactly known, but it is quite possible that the difference may be the result of the presence of HEDS in ECAP-8 Fe, which may lead to an enhancement in boundary diffusivity.

Experimentally, the enhancement of GB diffusivity due to the existence of non-equilibrium GBs was investigated recently by means of Cu diffusion in coarse-grained Ni (d = 20 μm), UFG Ni processed by ECAP ($d = 0.3$ μm), UFG Ni processed by ECAP and subsequently annealed at 523 K for 1 hour ($d = 0.3$ μm), and nanocrystalline Ni processed by electrolytic deposition ($d = 0.03$ μm).[26] It is observed that the GB diffusivity of Cu in UFG Ni processed by ECAP is more than two orders of magnitude higher than that in nanocrystalline Ni processed by electrolytic deposition. Moreover, the activation energy of the GB diffusion of Cu in UFG Ni processed by ECAP was found to be about 3 times lower than that in coarse-grained Ni. The enhancement of Cu GB diffusivity and the low activation energy in UFG Ni processed by ECAP was also attributed to the existence of nonequilibrium GBs, rather than to the refinement of grain sizes.

It appears that although the HEDS associated with the saturation of dislocations in UFG materials processed by means of severe plastic deformation leads to high strengthening, it is harmful to ductility. A slight annealing, which evolves HEDS into LEDS without causing grain growth, will lead to a better ductility and toughness without losing strength. The benefit of subsequent annealing at low temperatures was also revealed in a low-carbon steel, which was subjected to ECAP for four passes at a temperature of 623 K.[9] A high yield strength of 937 MPa and a UTS of 943 MPa were observed. The existence of almost no work hardening between yield stress and UTS in the as-pressed steel was attributed to the nonequilibrium GBs with high internal stresses. As expected, after annealing at 753 K for 24 hours, a high portion of equilibrium GBs and a lower density of dislocations accompanied with slight grain growth in ferrite grains were observed, leading to a better ductility with a slight reduction of strength.

The improved work hardening and better ductility after annealing were also observed in a pure Ti processed by ECAP for eight passes, followed by cold extrusion for a reduction in cross-sectional area of 75 pct.[27] A high tensile strength of the as-processed Ti was achieved, but strain softening occurred after a brief work hardening. After annealing at 573 K for half an hour, GBs are clearly defined without significant grain growth. The work-hardening region was greatly extended and the ductility was much improved without significantly decreasing the ultimate strength.

Most recently, a significantly improved work hardening was achieved by a brief annealing at 473 K of an UFG pure Cu.[28] The UFG Cu processed by rolling at liquid nitrogen temperature to a high value of percentage cold work (93 pct) can reach a high strength, but without a work-hardening region; therefore, it possesses short elongation. After a brief annealing at 473 K for 3 minutes, a bimodal UFG microstructure was formed, leading to a pronounced work-hardening capacity with a combination of high strength and high ductility in the UFG pure Cu that is 6 times stronger (a yield

stress in excess of 400 MPa) than normal, without significant loss of ductility (65 pct elongation to failure).

V. CONCLUSIONS

The evolution of dislocations of pure Fe during ECAP was investigated and correlated with the mechanical properties. Intensive dislocation-cell blocks are observed after one pass and even more in the subsequent pressings. The low-energy dislocation cell blocks may have changed into the high-energy dislocation structures in the final several pressings. The high density array of dislocations plays a significant role in strengthening. The high-energy dislocation structures may cause the materials to lose work-hardening ability and show a cleavage morphology of fracture surface. A proper subsequent annealing treatment will lead to the evolution of high-energy dislocation structures to low-energy dislocation structures, while maintaining little grain growth, which allows ultrafine-grained materials to achieve an excellent combination of high strength and high ductility with the dimpled fracture surface.

ACKNOWLEDGMENTS

This work is supported by the Army Research Office under Grant Nos. DAAD19-01-1-0627 and DAAD19-03-1-0020. The ECAP was performed at the University of Southern California by BH, who expresses his appreciation to Professor T.G. Langdon. The technical support of the operation of TEM from Dr. W.A. Chiou is gratefully acknowledged.

REFERENCES

1. R.Z. Valiev, R.K. Islamgaliev, and I.V. Alexandrov: *Progr. Mater. Sci.*, 2000, vol. 45, pp. 103-89.
2. E. Ma: *Powder. Metall.*, 2000, vol. 43, pp. 306-10.
3. T.S. Srivatsan, E.J. Lavernia, and F.A. Mohamed: *Int. J. Powder Metall.*, 1990, vol. 26, pp. 321-34.
4. G. Langford and M. Cohen: *Trans. ASM*, 1969, vol. 62, pp. 623-38.
5. D.A. Hughes and N. Hansen: *Acta Mater.*, 1997, vol. 45, pp. 3871-86.
6. R.Z. Valiev, Y.V. Ivanisenko, E.F. Rauch, and B. Baudelet: *Acta Mater.*, 1996, vol. 44, pp. 4705-12.
7. R.K. Islamgaliev, N.F. Yunusova, I.N. Sabirov, A.V. Sergueeva, and R.Z. Valiev: *Mater. Sci. Eng.*, 2001, vols. A319–A321, pp. 877-81.
8. D.H. Shin, B.C. Kim, Y.-S. Kim, and K.T. Park: *Acta Mater.*, 2000, vol. 48, pp. 2247-55.
9. K.T. Park, Y.S. Kim, J.G. Lee, and D.H. Shin: *Mater. Sci. Eng.*, 2000, vol. A293, pp. 165-72.
10. D.H. Shin, I. Kim, J. Kim, and K.-T. Park: *Acta Mater.*, 2001, vol. 49, pp. 1285-92.
11. D.H. Shin, J.J. Pak, Y.K. Kim, K.-T. Park, and Y.S. Kim: *Mater. Sci. Eng.*, 2002, vol. A325, pp. 31-37.
12. Y. Fukuda, K. Oh-ishi, Z. Horita, and T.G. Langdon: *Acta Mater.*, 2002, vol. 50, pp. 1359-68.
13. B.Q. Han, E.J. Lavernia, and F.A. Mohamed: *Metall. Mater. Trans. A*, 2003, vol. 34A, pp. 71-83.
14. T.G. Nieh, J. Wadsworth, C.T. Liu, G.E. Ice, and K.S. Chung: *Mater. Trans.*, 2001, vol. 42, pp. 613-18.
15. T.R. Malow and C.C. Koch: *Acta Mater.*, 1998, vol. 46, pp. 6459-73.
16. N. Hansen: *Mat. Sci. Technol.*, 1990, vol. 6, pp. 1039-47.
17. D. Kuhlmann-Wilsdorf: *Phil. Mag. A*, 1999, vol. 79, pp. 955-1008.
18. D. Kuhlmann-Wilsdorf: *Metall. Mater. Trans. A*, 2002, vol. 33A, pp. 2519-39.
19. V.M. Segal: *Mater. Sci. Eng.*, 1995, vol. A197, pp. 157-64.
20. J.Y. Huang, Y.T. Zhu, H. Jiang, and T.C. Lowe: *Acta Mater.*, 2001, vol. 49, pp. 1497-1505.
21. A.A. Nazarov, A.E. Romanov, and R.Z. Valiev: *Acta Metall. Mater.*, 1993, vol. 41, pp. 1033-40.
22. C.H. Moelle and H.J. Fecht: *Nanostruct. Mater.*, 1995, vol. 6, pp. 421–24.
23. T.H. Courtney: *Mechanical Behavior of Materials*, 2nd ed., McGraw-Hill Higher Education, New York, NY, 2000.
24. H.J. Frost and M.F. Ashby: *Deformation-Mechanism Maps: The Plasticity and Creep of Metals and Ceramics*, Pergamon Press, New York, NY, 1982.
25. R.Z. Valiev, E.V. Kozlov, Y.F. Ivanov, J. Lian, A.A. Nazarov, and B. Baudelet: *Acta Metall. Mater.*, 1994, vol. 42, pp. 2467-75.
26. Y.R. Kolobov, G.P. Grabovetskaya, M.B. Ivanov, A.P. Zhilyaev, and R.Z. Valiev: *Scripta Mater.*, 2001, vol. 44, pp. 873-78.
27. V.V. Stolyarov, Y.T. Zhu, T.C. Lowe, and R.Z. Valiev: *Mater. Sci. Eng.*, 2001, vol. A303, pp. 82-89.
28. Y. Wang, M. Chen, F. Zhou, and E. Ma: *Nature*, 2002, vol. 419, pp. 912-15.